Near-infrared Electrochromic Behavior of Dibenzothiepin Derivatives Attached by Two Michler's Hydrol Blue Units

Yusuke Ishigaki,*[a] Masaki Takata,[a] Takuya Shimajiri,[a,b] Luyan Wu,[c] Wenhui Zeng,[c] Deju Ye,[c] and Takanori Suzuki*[a]

[a] Prof. Dr. Y, Ishigaki, Mr. M. Takata, Dr. T. Shimajiri, Prof. Dr. T. Suzuki
Department of Chemistry, Faculty of Science, Hokkaido University
N10 W8, North-ward, Sapporo 060-0810, Japan
E-mail: yishigaki@sci.hokudai.ac.jp
tak@sci.hokudai.ac.jp

[b] Dr. T. Shimajiri,
Creative Research Institution, Hokkaido University,
N21 W10, North-ward, Sapporo, Hokkaido 001-0021, Japan.

[c] Dr. L. Wu, Ms. W. Zeng, Prof. Dr. D. Ye
State Key Laboratory of Analytical Chemistry for Life Science, School of Chemistry and Chemical Engineering, Nanjing University
Nanjing 210023, China

Supporting information for this article is given via a link at the end of the document.

Dedication: *In memory of Siegfried Hünig*

Abstract:

10,11-Bis[bis(4-dimethylaminophenyl)methylene]dibenzo[*bf*]thiepin (**1**) and -oxepin (**2**) were prepared as stable yellow crystalline compounds, which are the cyclic analogues of electron-donating hexaarylbutadienes. Upon two-electron oxidation, they are reversibly transformed into the title dications ($\mathbf{1}^{2+}$ and $\mathbf{2}^{2+}$) exhibiting near-infrared (NIR) absorptions, which were also isolated as stable salts. These redox pairs can serve as new entries into less well-explored organic NIR-electrochromic systems, and the separation of redox peaks (electrochemical bistability) was attained for $\mathbf{1}/\mathbf{1}^{2+}$ and $\mathbf{2}/\mathbf{2}^{2+}$, thanks to drastic geometrical changes between neutral and dicationic states, as revealed by a series of X-ray analyses. Thiepin-*S,S*-dioxide analogue ($\mathbf{3}/\mathbf{3}^{2+}$) exhibits quite similar redox behavior due to nonaromatic nature of the dibenzothiepin or -oxepin unit in $\mathbf{1}^{2+}$ and $\mathbf{2}^{2+}$, whereas thiepin-*S*-oxide derivative ($\mathbf{4}/\mathbf{4}^{2+}$) does not exhibit bistability due to the less change in geometry upon electron transfer, showing that a subtle change of a bridging atom in the central seven-membered ring can modify the redox properties.

Introduction

Electrochromic material (EM), in which the electric potential as an input is transduced into the color change as an output (electrochromism) have recently attracted considerable attention.[1] They have been widely used in the development of auto-dimming mirrors, smart windows and displays.[2] Organic π-conjugating systems called violene/cyanine hybrids[3] are a representative class of EM. In these molecules, two-electron (2e) transfer at nearly the same potential induces the formation of two cyanine units at the termini of the linearly conjugating π-system. Our studies on the electron-donating hexaarylbutadienes[4, 5] have shown that 1,1,4,4-tetrakis(4-dimethylaminophenyl)-2,3-diarylbutadienes (**I**)[4] can be classified as violene/cyanine hybrids since Michler's Hydrol Blue (MHB)[6] units in $\mathbf{I}^{2+}$ are also a cyanine-type conjugating system (Scheme 1).

A striking feature of the EM pair of $\mathbf{I}/\mathbf{I}^{2+}$ is a vivid color change from pale yellow to deep violet. Dication $\mathbf{I}^{2+}$ exhibits strong absorption in the near-infrared (NIR) region ($\lambda > 700$ nm). Only a limited number of such NIR-EM have been reported so far,[7] and the absence of heavy metals is favorable for their use in biological applications. For this purpose, the hexaarylbutadiene framework of $\mathbf{I}/\mathbf{I}^{2+}$ can serve as a very versatile platform because the redox potentials for a color change as well as the NIR-absorption wavelength can be modified systematically by attaching the proper substituents.[5] Finally, the stability of $\mathbf{I}^{2+}$ under aqueous/physiological conditions enabled us to make use of these EM to create a NIR-bioimaging protocol by targeting the redox species in biological systems (e.g., hydrogen sulfide as a reductant and hydroxy radical as an oxidant).[8]

In addition to the color change, a drastic change in geometry is also observed during the redox interconversion between **I** and $\mathbf{I}^{2+}$. Such a structural change is often obseved with electrochemical bistability ("dyrex" behavior),[9] based on the difference between the oxidation potential of the neutral species and the reduction potential of the dicationic species, as seen in dihydrophenanthrene-type compounds (*vide infra*).[10] However, for the pair $\mathbf{I}/\mathbf{I}^{2+}$, no bistability was observed, probably due to the structural flexibility that accompanies the adoption of readily interconverting s-*cis*/s-*trans* forms for **I** and *E*/*Z* forms for $\mathbf{I}^{2+}$, respectively.

For the further development of the sophisticated bioimaging protocols, there is a need for new NIR-EM endowed with electrochemical bistability, so that the reverse electron-transfer can be suppressed after the reaction of EM with the biological redox species. Here we designed the first cyclic derivatives of hexaarylbutadiene-type NIR-EM ($\mathbf{1}/\mathbf{1}^{2+}$ and $\mathbf{2}/\mathbf{2}^{2+}$) with bridging atoms of S and O, respectively (Scheme 2).

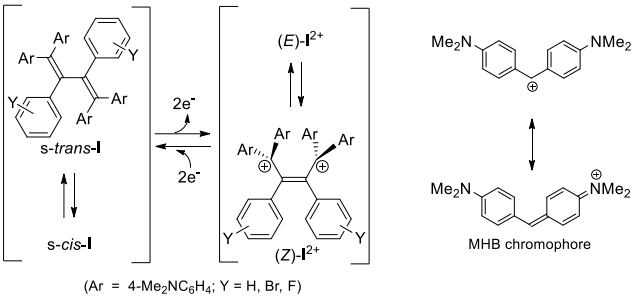

Scheme 1. Hexaarylbutadiene-type NIR-EM $\mathbf{I}/\mathbf{I}^{2+}$ undergoing facile conformational/configurational changes.

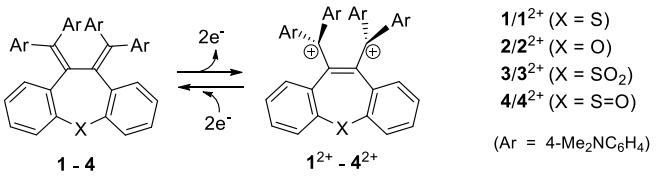

Scheme 2. Newly designed NIR-EMs ($\mathbf{1}/\mathbf{1}^{2+}$ - $\mathbf{4}/\mathbf{4}^{2+}$) with a seven-membered ring of increased geometrical rigidity.

The central seven-membered ring system would provide partial geometric rigidity, and thus the newly designed NIR-EM pairs would exhibit electrochemical bistability. This paper reports their preparation and redox and electrochromic properties, and discusses their electrochemical bistability based on their X-ray structures and optimized geometries by DFT calculations.

Results and Discussion

Molecular design. In our previous work on redox active quinodimethanes,[11] two MHB units were generated at the 9,10-positions of anthracene upon 2e-oxidation of 11,11,12,12-tetrakis(4-dimethylaminophenyl)-9,10-anthraquinodimethane (**II**), which is a butterfly-shaped deformed molecule, whereas the corresponding dication (**II**$^{2+}$) adopts a twisted geometry around the exocyclic bond (twisting angle: 72.9°) (Scheme 3a). Due to the drastic change in geometry, there is a large separation (ΔE: 0.71 V) between the oxidation potential of **II** (+0.47 V vs SCE in CH_2Cl_2) and the reduction potential of **II**$^{2+}$ (-0.24 V), which gives electrochemical bistability. On the other hand, the NIR absorption is less prominent in **II**$^{2+}$ since its absorption-end is at around 700 nm due to less interaction between two MHB units.[12]

Dication **III**$^{2+}$ with two MHB units at the vicinal 9,10-positions of phenanthrene has an electronic structure more similar to that of **I**$^{2+}$, thus exhibiting NIR absorption. However, its reduced form, 11,11,12,12-tetrakis(4-dimethylaminophenyl)-9,10-phenanthraquinodimethane (**III**),[13] was proven to be too unstable to handle (Scheme 3b) although the related phenanthraquinodimethane with less donating aryl groups can be isolated, which interconverts reversibly while exhibiting electrochemical bistability (ΔE: 0.50 V for 4-methoxyphenyl derivative **IV**/**IV**$^{2+}$).[10] The instability of **III** may be due to the confinement of strongly electron-donating diene moieties in the rigid six-membered ring, as well as the partial contribution from the diradical form **III**$^{2\bullet}$ with a phenanthrene skeleton (*vide infra*). We have designed the NIR-EM **1**/**1**$^{2+}$ and **2**/**2**$^{2+}$ (X = S and O, respectively) containing a seven-membered ring in the center of the skeleton to reduce the proximity of the dimethylaniline nuclei by being less planar and to diminish the diradical character by being nonaromatic. At the same time, the bridging atom in the seven-membered ring can be used to finely tune the redox properties of the new series of NIR-EM pairs, which is demonstrated by studying **3**/**3**$^{2+}$ and **4**/**4**$^{2+}$, which have the different bridging atoms (SO_2 and S=O, respectively).

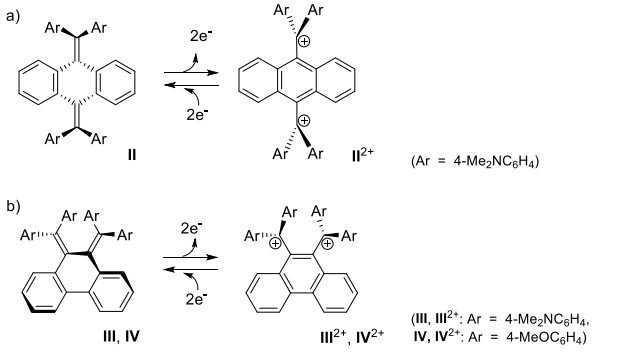

Scheme 3. a) Anthraquinodimethane-type and b) phenanthraquinodimethane-type EMs with electrochemical bistability. Electrochromic behavior in the NIR region could not be attained in both motifs due to less conjugation of MHB units in **II**$^{2+}$, the less stability in **III**, and less red-shifted absorption in **IV**$^{2+}$.

Preparation of neutral dienes (1 - 4). Oxidative dimerization[14] has been used as a common synthetic route to obtain electron-donating hexaarylbutadienes,[4,5] and thus newly designed donors with a seven-membered ring would be obtained by oxidative cyclization of bis(triarylethene)s connected by a bridging atom (Scheme 4). Actually, as the precursors of **1**, **2**, and **3**, bis[(diarylethenyl)phenyl] sulfide **5**, bis[(diarylethenyl)phenyl] ether **6**, and bis[(diarylethenyl)phenyl] sulfide-*S,S*-dioxide **7** were selected, which are readily obtained from the corresponding dialdehydes[15] by the double Horner–Wadsworth–Emmons reaction[16] using $Ar_2CHPO(OEt)_2$.[17] Upon oxidation of **5** - **7** with $(4\text{-}BrC_6H_4)_3N^{+\bullet}SbCl_6^-$ (magic blue, MB), dicationic species of **1**$^{2+}$ - **3**$^{2+}$ were generated, from which the target neutral donors **1** - **3** were obtained upon reduction with Zn. For the preparation of sulfoxide (**4**), thiepin-type dication **1**$^{2+}$ was oxygenated with *m*-chloroperbenzoic acid (*m*CPBA) to give **4**$^{2+}$, which was converted to donor **4** by reduction with Zn. All of the neutral donors **1** - **4** are stable pale-yellow crystalline substances.

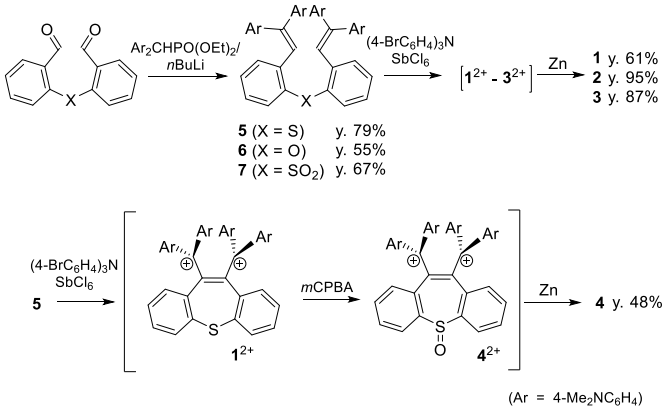

Scheme 4. (a) Preparation of **1** - **3** via oxidative cyclization of bis(triarylethene) derivatives. (b) Preparation of sulfoxide **4** through *m*CPBA oxygenation of dicationic thiepin **1**$^{2+}$.

Redox behavior of 1/1^{2+} and 2/2^{2+}.
Upon treatment of thiepin **1** with 2 equivalents of MB in CH_2Cl_2, **1**$^{2+}$$(SbCl_6^-)_2$ was isolated as a dark blue powder in 98% yield. The dication exhibits a strong absorption at 641 nm (ε 51700) in CH_2Cl_2 with an extended absorption-end at around 850 nm, whereas neutral **1** has absorptions mainly in the UV region [369 nm (ε 21500)]. This dication salt regenerated **1** in 98% yield by Zn-reduction in MeCN. Similarly, oxepin **2** [350 nm (sh) (ε 26000)] and **2**$^{2+}$$(SbCl_6^-)_2$ [646 nm (ε 56100)] were interconverted in high isolated yield (oxidation: 97% yield, reduction: 97% yield, respectively), thus showing that the newly prepared NIR-EM pairs (**1**/**1**$^{2+}$ and **2**/**2**$^{2+}$) exhibit high reversibility.

On the other hand, according to voltammetric analyses in CH_2Cl_2, **1** and **2** exhibit irreversible 2e-oxidation waves with a largely shifted return peak in the cathodic region, which corresponds to 2e-reduction of the corresponding dication (Figure 1). Thus, the oxidation potential of **1** is +0.62 V vs SCE (Pt electrode, scan rate of 100 mV s^{-1}) whereas the reduction potential of **1**$^{2+}$ is +0.14 V, which reflects electrochemical bistability with ΔE of 0.48 V. A quite similar voltammogram was observed for the pair of **2** (E^{ox}: +0.53 V) and **2**$^{2+}$ (E^{red}: +0.06 V). These results are in sharp contrast to those for hexaarylbutadiene-type donors without bistability [e.g., **I**/**I**$^{2+}$ (Y= H): E^{ox} = E^{red} = +0.25 V], and thus bistability in the present EMs is endowed by incorporation of a seven-membered ring.

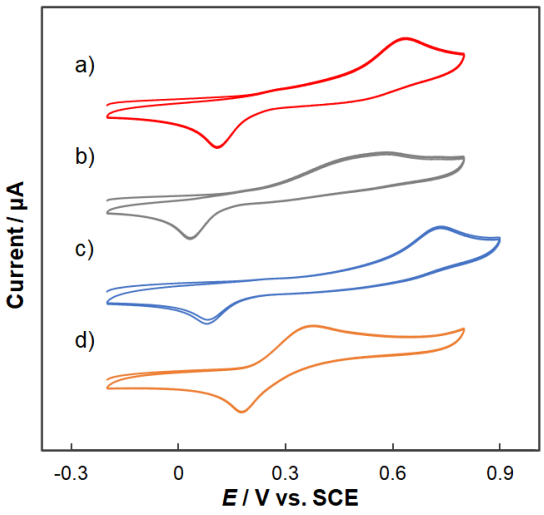

Figure 1. Cyclic voltammograms of (a) **1**, (b) **2**, (c) **3**, and (d) **4** in CH_2Cl_2 containing 0.1 M Bu_4NBF_4 as a supporting electrolyte. (*E*/V vs SCE, scan rate 100 mV s^{-1}, Pt electrodes). E^{ox} and E^{red} are calculated as E_{peak}(anode) – 0.03 and E_{peak}(cathode) + 0.03, respectively. Under the similar conditions, the oxidation potential of ferrocene is +0.53 V.

X-ray analyses of 1, $1^{2+}(SbCl_6^-)_2$, 2 and $2^{2+}(SbCl_6^-)_2$. In many dyrex systems that exhibit electrochemical bistability with a large separation of redox peaks, a drastic difference in geometry has been observed for neutral and charged species. To investigate the origin of electrochemical bistability for the present EMs, a series of X-ray analyses were conducted.

The 10,11-dihydrodibenzothiepin skeleton of **1** adopts a twisted-chair conformation. In this geometry, the conjugated tetraarylbutadiene unit has a large torsion angle (θ) of 75.8(5)° for <C_{9a}-C_{10}-C_{11}-C_{11a}, whereas both diarylmethylene units are nearly planar [dihedral angle (χ): 5.1(1) and 8.6(1)°] with normal bond length (d_x) [1.356(2) and 1.357(2) Å] (Table 1). The sulfide plane defined by the three atoms of C_{4a}-S-C_{5a} is nearly coplanar to each side of adjacent benzene rings [dihedral angle (ϖ): 3.0(1) and 32.6(1)°] (Figure 2a). The large θ and small ϖ values are characteristic of the twisted-chair conformation.

In contrast, in the crystal of $\mathbf{1}^{2+}(SbCl_6^-)_2$, the central seven-membered ring adopts a tub-boat form, and thus the sulfide plane of C_{4a}-S-C_{5a} has quite large dihedral angles with the adjacent benzene rings [ϖ: 61.6(1) and 62.4(3)°], while the torsion angle for <C_{9a}-C_{10}-C_{11}-C_{11a} is quite small [θ: 9.7(1)°]. Furthermore, the central C_{10}-C_{11} bond length (d_c) becomes much smaller [1.358(10) Å] than that in the neutral **1** [1.500(2) Å], while the exocyclic bonds become longer [d_x: 1.489(10) and 1.509(10) Å]. The observed bond lengths are those of the typical butene-1,4-diyl dication. The large twisting angles for the exocyclic bonds [χ: 66.5(4) and 72.1(3)°] are in accord with their single-bond character (Figure 2b). Such a drastic structural change between **1** (twisted-chair) and $\mathbf{1}^{2+}$ (tub-boat) can explain the observed electrochemical bistability for the EM pair of $\mathbf{1}/\mathbf{1}^{2+}$, and the key feature is the conformational variance of the seven-membered ring that affects the 1,3-butadiene/2-butene-1,4-diyl geometry.

Similar changes were observed when comparing the X-ray structures of oxepin derivatives **2** (twisted-chair: large θ and small ϖ) and $\mathbf{2}^{2+}(SbCl_6^-)_2$ (tub-boat: small θ and large ϖ) (Table 1). The observed change in geometry upon 2e-transfer again explains the electrochemical bistability of $\mathbf{2}/\mathbf{2}^{2+}(SbCl_6^-)_2$ pair as in $\mathbf{1}/\mathbf{1}^{2+}(SbCl_6^-)_2$.

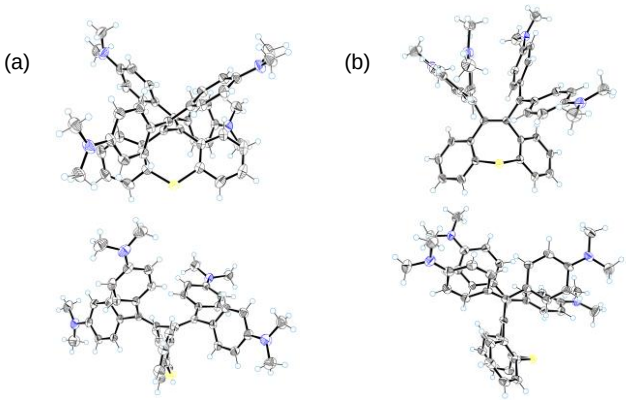

Figure 2. (a) Two views of ORTEP drawing of thiepin **1** and (b) the dication salt $\mathbf{1}^{2+}(SbCl_6^-)_2$ (MeCN solvate) determined by X-ray at 150 K. Thermal ellipsoids are shown at the 50% probability level.

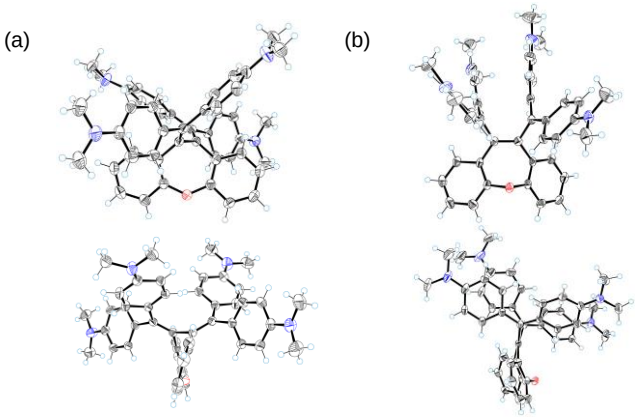

Figure 3. (a) Two views of ORTEP drawing of oxepin **2** and (b) the dication salt $\mathbf{2}^{2+}(SbCl_6^-)_2$ determined by X-ray at 150 K. Thermal ellipsoids are shown at the 50% probability level. The geometrical data of $\mathbf{2}/\mathbf{2}^{2+}(SbCl_6^-)_2$ are shown in Table 1.

Table 1. Selected structural parameters determined by X-ray analyses.

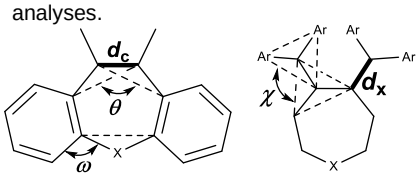

twisted-chair: large θ, small ω

tub-boat: small θ, large ω

compound	θ/°	ω/°	χ/°	d_c/Å	d_x/Å
1	75.8(5)	3.0(1)	5.1(1)	1.500(2)	1.356(2)
[X = S]		32.6(1)	8.6(1)		1.357(2)
2	92.3(5)	10.8(1)	1.4(1)	1.500(2)	1.352(2)
[X = O]		16.7(1)	3.9(1)		1.354(2)
3	83.8(3)	15.8(2)	1.8(2)	1.499(5)	1.349(6)
[X = SO_2]		40.8(2)	7.0(2)		1.352(5)
4	23.9(3)	61.0(1)	8.4(1)	1.492(3)	1.346(3)
[X = S=O]		70.1(1)	16.1(1)		1.371(3)
$\mathbf{1}^{2+}(SbCl_6^-)_2$	9.7(1)	61.6(1)	66.5(4)	1.358(10)	1.489(10)
[X = S]		62.4(3)	72.1(3)		1.509(10)
$\mathbf{2}^{2+}(SbCl_6^-)_2$	12.8(1)	65.8(3)	65.0(2)	1.362(6)	1.497(6)
[X = O]		72.4(3)	78.5(2)		1.505(6)
$\mathbf{3}^{2+}(SbCl_6^-)_2$	2.17(2)	57.4(1)	63.6(1)	1.362(4)	1.506(3)
[X = SO_2]		64.1(1)	68.4(1)		1.514(3)
$\mathbf{4}^{2+}(SbCl_6^-)_2$	1.64(1)	66.5(2)	62.5(2)	1.350(7)	1.494(6)
[X = S=O]		70.0(2)	69.1(2)		1.501(6)

DFT calculations for the nonaromatic nature of dibenzothiepin and dibenzoxepin rings in 1^{2+} and 2^{2+}. Thiepin and oxepin have attracted attention as antiaromatic compounds,[18] while the dibenzothiepin and dibenzoxepin units in 1^{2+} and 2^{2+} would not be considered to be antiaromatic despite the formal 16π-electron systems due to their nonplanar tub-boat geometry. Based on single-point DFT calculations[19] using the X-ray geometries B3LYP/6-31+G(d), we confirmed that the dibenzothiepin and dibenzoxepin units are nonaromatic.

For the nucleus-independent chemical shifts [NICS(n)zz][20] calculation, a rectangular plane is defined by C_{4a}, C_{5a}, C_{9a}, and C_{11a} to represent the nonplanar seven-membered ring. The NICS(n)zz values of 1^{2+} exhibit considerable variation (–0.692, –2.64, +10.9, +14.8, and +0.100 for n = 2, 1, 0, -1, and -2, respectively), showing that these values are not intrinsic to the seven-membered ring, but rather are affected by the neighboring benzene rings. Actually, as shown in Figure 4a, the iso-chemical shielding surface in the Z direction (ICSSzz)[21] clearly shows that the calculated chemical shielding in the seven-membered ring is largely affected by those of fused benzene rings. This holds true for 2^{2+} [NICS(n)zz = –1.00, +0.165, +19.3, +14.0, and –1.66 for n = 2, 1, 0, -1, and -2, respectively] with the similar ICSSzz (Figure 4b).

Finally, nonaromaticity of the tricyclic core was confirmed by plots of anisotropy of the induced current density (AICD),[22] showing that almost no ring-current is present in the seven-membered ring in 1^{2+} and 2^{2+} (Figure 5). The nonplanarity and nonaromaticity of the central seven-membered ring is important for stabilizing the neutral forms of **1** and **2** by reducing the diradical character ($1^{2\bullet}$ and $2^{2\bullet}$),[23] which is the major issue for the six-membered analogue **III**, since planarity and formation of aromaticity of the central ring in $\mathbf{III}^{2\bullet}$ facilitates the diradical character (Scheme 5).[24] To confirm this explanation, further studies were conducted on the redox pair of $\mathbf{3}/\mathbf{3}^{2+}$, in which the bridging atom of SO_2 warrants a nonaromatic character of the seven-membered ring. Once the redox properties of $\mathbf{3}/\mathbf{3}^{2+}$ were proven to be similar to those of $\mathbf{1}/\mathbf{1}^{2+}$, the nonaromatic nature of the dibenzothiepin unit in the present EM could be demonstrated experimentally.

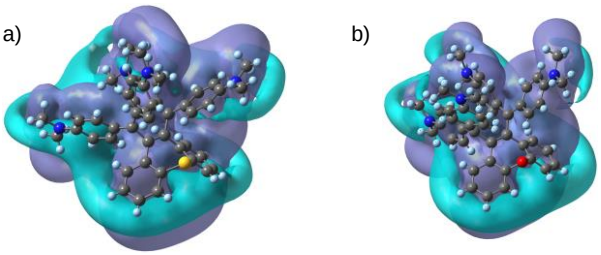

Figure 4. Iso-chemical shielding surface in the Z direction obtained with the gauge-independent atomic orbital method for (a) 1^{2+} and (b) for 2^{2+} (isovalue = 2) .

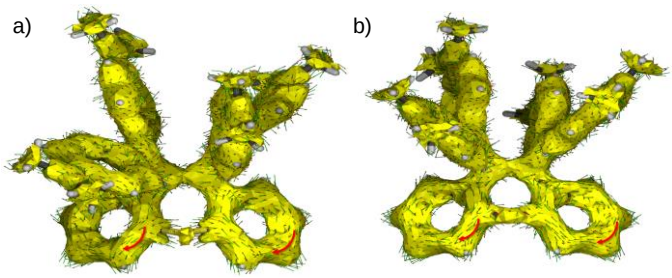

Figure 5. Plots of anisotropy of the induced current density (AICD) of (a) 1^{2+} and (b) 2^{2+}.

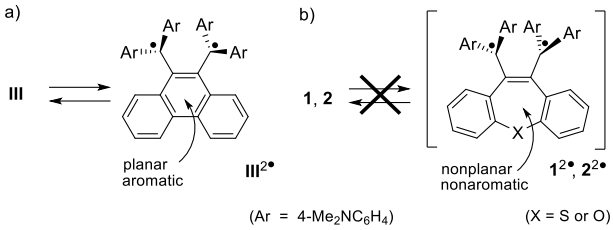

Scheme 5. Equilibrium with diradical form in (a) 9,10-dihydrophenanthrene-type diene (**III**) and non-equilibrium in (b) 10,11-dihydrodibenzo[*bf*]thiepin and -oxepin (**1** and **2**), due to different geometrical feature and aromatic nature of the central ring system.

Redox properties and X-ray analyses of 3 and $\mathbf{3}^{2+}(SbCl_6^-)_2$. A voltammetric analysis shows that **3** with a SO_2 bridging atom exhibits electrochemical bistability [E^{ox}: +0.72 V, E^{red}: +0.06 V, and ΔE: 0.66 V] (Figure 1c), which is similar to the cases of thiepin and oxepin derivatives, **1** and **2**. Actually, **3** [λ_{max} (CH_2Cl_2): 363 nm (ε 26100)] was found to be interconvertible with $\mathbf{3}^{2+}(SbCl_6^-)_2$ [659 nm (ε 64800)] in high isolated yields upon treatment with MB and Zn (oxidation: 98% yield, reduction: 98% yield, respectively).

X-ray analysis of **3** shows that its twisted-chair conformation is quite similar to those of **1** and **2** (Figure 6a). In addition, the crystal of $\mathbf{3}^{2+}(SbCl_6^-)_2$ has a tub-boat-form dication that resembles 1^{2+} and 2^{2+} (Figure 6b). In this way, the electrochemical bistability observed in another NIR-EM pair of $\mathbf{3}/\mathbf{3}^{2+}$ is endowed by the drastic change in structure upon 2e-electron transfer.

The slightly higher E^{ox} value of **3** compared to those of **1** and **2** can be explained by the electron-withdrawing nature of the bridging SO_2 group, which was verified by the HOMO level calculated using the DFT method [B3LYP/6-31G(d)]: –4.23, –4.21, and –4.45 eV for **1** – **3**, respectively (Table S1). All molecules were optimized as the twisted-chair conformation as the global-minimized structure, which are similar to the X-ray structures. In addition, the DFT calculations showed another set of optimized geometries for **1** – **3** with a tub-boat conformation, which are higher in energy than the corresponding twisted-chair conformers by 5.75, 5.99, and 3.52 kcal mol^{-1}, respectively. On the other hand, **4** with a S=O bridge has an optimized structure, in which the tub-boat conformer is more stable than the twisted-chair by 0.94 kcal mol^{-1}, and the characteristic feature is that the HOMO-LUMO gap is smaller (3.09 eV) than that of the twisted-chair form (3.60 eV).

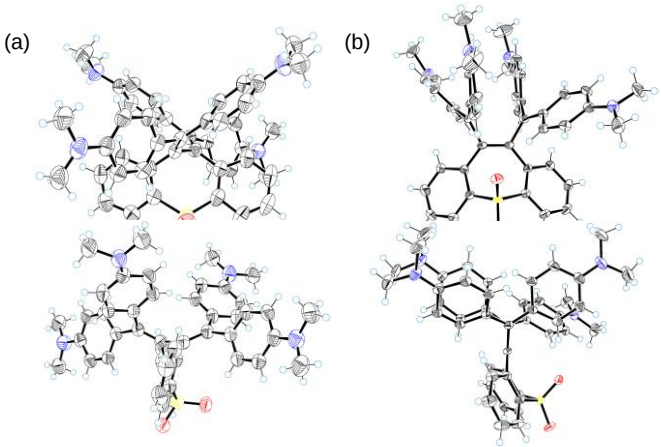

Figure 6. (a) Two views of ORTEP drawing of thiepin-*S*,*S*-dioxide **3** and (b) the dication salt $\mathbf{3}^{2+}(SbCl_6^-)_2$ determined by X-ray at 150 K. Thermal ellipsoids are shown at the 50% probability level. The geometrical data of $\mathbf{3}/\mathbf{3}^{2+}(SbCl_6^-)_2$ are shown in Table 1.

Redox properties and X-ray analyses of 4 and $4^{2+}(SbCl_6^-)_2$. To investigate the effects of a subtle change of the bridging atom (X: S, SO_2, S=O) on the redox properties of the NIR-EMs, further studies were conducted. As in other pairs studied in this work, **4** [λ_{max} (CH_2Cl_2): 433 nm (ε 7500)] and $\mathbf{4}^{2+}(SbCl_6^-)_2$ [661 nm (ε 69600)] could be interconverted in high isolated yields upon treatment with MB and Zn (oxidation: 97% yield, reduction: 98% yield, respectively). According to the X-ray analysis of **4**, the molecule adopts the tub-boat conformation, as shown by the small θ and large ϖ values, which is rather different from the twisted-chair form of **1** – **3** but consistent with the prediction from the DFT calculation (Figure 7a). Unlike **1** – **3**, **4** exhibits an outstanding absorption band in the visible region with extended absorption-end at around 530 nm, which is characteristic of the tub-boat conformation with a smaller HOMO-LUMO gap (Figure S2).

Detailed examination of the X-ray geometry indicated that there is a transannular interaction between one of the electron-rich exocyclic double bonds and the electron-deficient S=O group in this tub-boat conformation. The interatomic distance of C_{12}=C_{10} ••• S=O [2.842(2) Å] is much smaller than the sum of the van der Waals radii of C (1.70 Å) and S (1.80 Å).[25] The angles for C_{12}=C_{10} ••• S and C_{10} ••• S=O [96.3(1)° and 165.8(1), respectively] are suitable for intramolecular π-donation from the π-orbital of the double bond to the σ hole on S of the S=O group (Figure 8a). The greater S=O bond length [1.488(2) Å] than those in **3** (X = SO_2) [1.433(3) and 1.425(3) Å] is in accord with the contribution from the zwitterionic form.

According to the single-point DFT calculation (B3LYP/6-31G*) using the crystal coordinates of **4**, the σ hole of S is clearly seen in the map of electrostatic potential (Figure 8b). Furthermore, natural bond orbital (NBO) analysis[26] showed that the intramolecular interaction between the anti-bonding orbital of S=O and the π orbital of C=C induces the second-order perturbation stabilization of 1.67 kcal mol^{-1}. In this way, it is likely that the observed transannular interaction is the key for switching the geometrical preference for the observed tub-boat form in **4**, because the suitable orbital arrangement is not possible in the twisted-boat geometry.

On the other hand, the dication molecule in $\mathbf{4}^{2+}(SbCl_6^-)_2$ adopts the tub-boat form similar to $\mathbf{1}^{2+}$ – $\mathbf{3}^{2+}$ salts. Consequently, the pair of $\mathbf{4/4}^{2+}$ does not undergo a change in geometry upon 2e-transfer, which is why electrochemical bistability is absent (E^{ox}: +0.29 V, E^{red}: +0.29 V) (Figure 1d). The less positive E^{ox} than those of **1** – **3** can be accounted for by the DFT calculation, which predicts a higher HOMO for the tub-boat form (**–**4.22 eV) than for the twisted-chair form (**–**4.45 eV) of **4**.

Electrochromic behavior in the NIR region for $\mathbf{1/1}^{2+}$, $\mathbf{2/2}^{2+}$, $\mathbf{3/3}^{2+}$ and $\mathbf{4/4}^{2+}$. Figure 9 shows the electrochromic behavior of the newly synthesized redox pairs. Upon constant-current electrochemical oxidation, new absorptions grow in the longer-wavelength region with the extended absorption-end over 800 nm with exhibiting deep blue color, which were assigned to the corresponding dications, as confirmed by comparisons with the spectra of the isolated $(SbCl_6^-)_2$ salt of the dications (Figure S2). These oxidation processes proceeded while exhibiting isosbestic point(s), showing the clean conversion of each redox pair. In all cases, high reversibility is confirmed by the spectral changes upon reduction process of the as-prepared dicationic species.

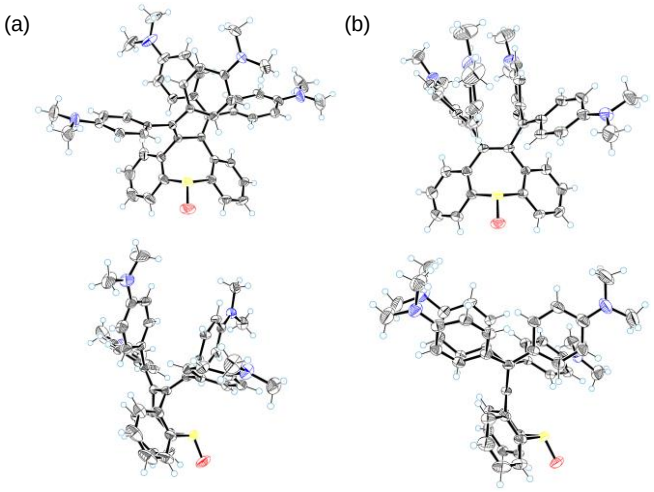

Figure 7. (a) Two views of ORTEP drawing of thiepin-*S*-oxide **4** (CH_2Cl_2 solvate) and (b) the dication salt $\mathbf{4}^{2+}(SbCl_6^-)_2$ determined by X-ray at 150 K. Thermal ellipsoids are shown at the 50% probability level. The geometrical data of $\mathbf{4/4}^{2+}(SbCl_6^-)_2$ are shown in Table 1.

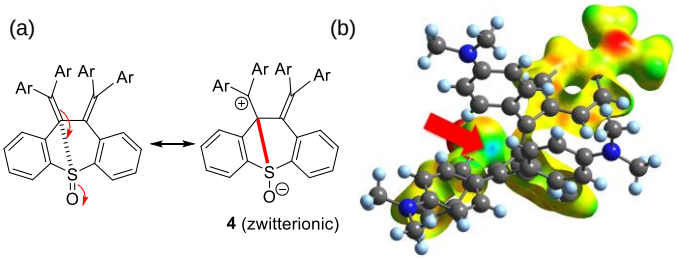

Figure 8. (a) Transannular interaction in **4**. (b) Electrostatic potential in **4** calculated by DFT method (isoval = 0.05). Red arrow indicates the σ-hole on S of S=O group.

Conclusion

In this work, the very rare examples[27] of organic NIR-EMs ($\mathbf{1/1}^{2+}$, $\mathbf{2/2}^{2+}$, and $\mathbf{3/3}^{2+}$) with electrochemical bistability have been successfully constructed, which were designed based on the dibenzothiepin, -oxepin, and thiepin-*S*,*S*-dioxide skeleton. The neutral forms adopt a twisted-chair geometry to reduce the steric repulsion of bis(diarylmethylene) units, as confirmed by experimentally (X-ray) and theoretically (DFT calculation). In contrast, for the dicationic states, two MHB chromophores are attached nearly perpendicularly to the central seven-membered ring with a tub-boat geometry. Such a drastic change in structure is the key to endow these NIR-EMs with a sufficient difference of redox potentials. DFT calculations also revealed that the central seven-membered rings in the dibenzothiepin and dibenzoxepin skeletons in $\mathbf{1}^{2+}$ and $\mathbf{2}^{2+}$ are nonaromatic, which is suitable for suppressing the diradical contribution in the neutral forms of **1** and **2**. Thus, the heteroatom on the seven-membered ring just gives the expected electronic effects affecting the HOMO level while modifying the oxidation potential of **1** - **3**. Due to the transannular interaction, thiepin-*S*-oxide **4** favors a tub-boat geometry similar to $\mathbf{4}^{2+}$. Thus, while the pair of $\mathbf{4/4}^{2+}$ does not exhibit bistability, it shows satisfactory electrochromism in the NIR region. These results may pave the way toward a new series of organic NIR-EMs, and a library of this category of compounds could be useful for the development of new bioimaging protocols.

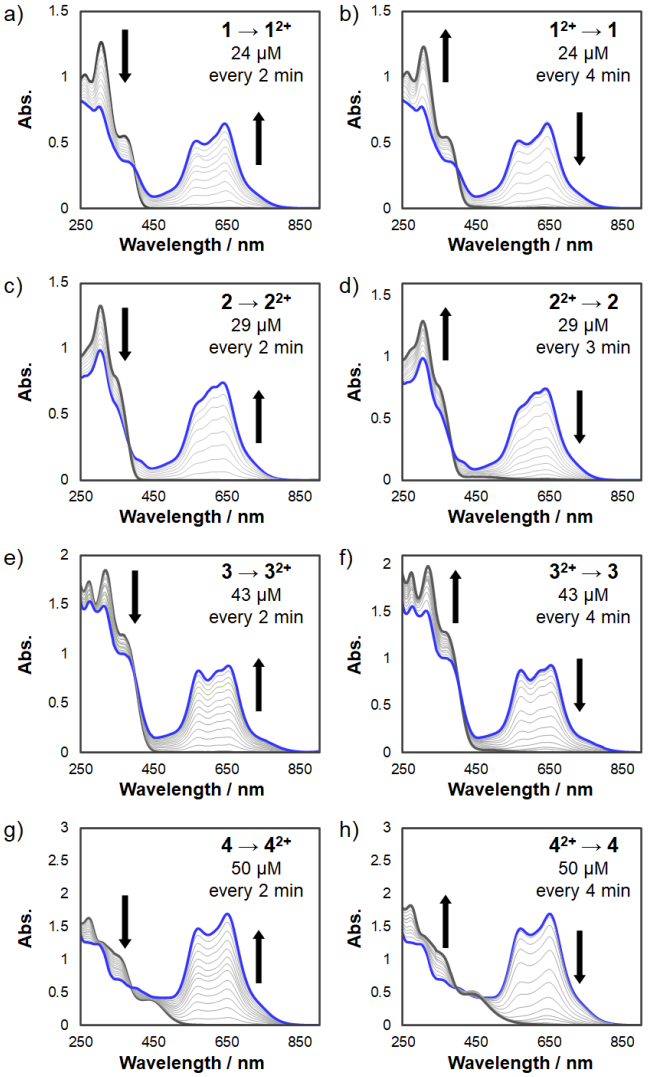

Figure 9. NIR electrochromic response of (a) **1**, (c) **2**, (e) **3**, and (g) **4** upon constant-current electrochemical oxidation (20 μA) and as-prepared dications (b) $\mathbf{1}^{2+}$, (d) $\mathbf{2}^{2+}$, (f) $\mathbf{3}^{2+}$, and (h) $\mathbf{4}^{2+}$ upon constant-current electrochemical reduction (20 μA) in CH_2Cl_2 containing 0.05 M Bu_4NBF_4 as a supporting electrolyte.

Acknowledgements

We thank Grant-in-Aid from MEXT and JSPS (Nos. 20H02719 and 20K21184 to TSu, and 21H01912 and 21H05468 to YI) Japan. This work was also supported by the Research Program of "Five-star Alliance" in "NJRC Mater. & Dev." MEXT.

Keywords: Redox chemistry • Cations • Cyclic voltammetry • Absorption • Dye

[1] a) P. Monk, R. Mortimer, D. Rosseinsky, *Electrochromism and Electrochromic Devices*, Cambridge University Press, Cambridge, **2007**. b) D. R. Rosseinsky, P. M. S. Monk, R. J. Mortimer, *Electrochromic Materials and Devices*, Wiley-VCH, Weinheim, Germany, **2013**. c) S. Mujawar, P. Patil, Electrochromism in Pristine and Doped Niobium Oxide Thin Films: Spray Pyrolytic *Synthesis of Niobium Oxide Thin Films for Smart Window Application*, LAP LAMBERT Academic Publishing, **2016**.

[2] a) R. J. Mortimer, *Annu. Rev. Mater. Res.* **2011**, *41*, 241. b) T. Xu, E. C. Walter, A. Agrawal, C. Bohn, J. Velmurugan, W. Zhu, H. J. Lezec, A. A. Talin, *Nat. Commun.* **2016**, *7*, 10479. c) C. Jing, Z. Gu, T. Xie, Y.-T. Long, *Chem. Sci.* **2016**, *7*, 5347–5351.

[3] a) S. Hünig, M. Kemmer, H. Wenner, I. F. Perepichka, P. Bäuerle, A. Emge, G. Gescheid, *Chem. Eur. J.* **1999**, *5*, 1969. b) S. Hünig, M. Kemmer, H. Wenner, F. Barbosa, G. Gescheidt, I. F. Perepichka, P. Bäuerle, A. Emge, K. Peters, *Chem. Eur. J.* **2000**, *6*, 2618.

[4] T. Suzuki, H. Higuchi, M. Ohkita, T. Tsuji, *Chem. Commun*. **2001**, 1574.

[5] Y. Ishigaki, T. Harimoto, K. Sugimoto, W. Lu, W. Zeng, D. Ye, T. Suzuki, *Chem. Asian J.* **2020**, *15*, 1147.

[6] S. F. Beach, J. D. Hepworth, P. Jones, D. Mason, J. Sawyer, G. Hallas, M. M. Mitchell, *J. Chem. Soc. Perkin Trans.* 2 **1989**, 1087

[7] a) G. A. Corrente, E. Fabiano, F. Manni, G. Chidichimo, G. Gigli, A. Beneduci, A.-L. Capodilupo, *Chem. Mater.* **2018**, *30*, 5610. b) Y. Okamoto, M. Tanioka, A. Muranaka, K. Miyamoto, T. Aoyama, X. Ouyang, S. Kamino, D. Sawada, M. Uchiyama, *J. Am. Chem. Soc.* **2018**, *140*, 17857. c) Q. Hao, Z.-J. Li, C. Lu, B. Sun, Y.-W. Zhong, L.-J. Wan, D. Wang, *J. Am. Chem. Soc.* **2019**, *141*, 19831. d) Z.-J. Li, C.-J. Yao, Y.-W. Zhong, *Sci. China Chem*. **2019**, *62*, 1675.e) Y. Ishigaki, H. Kawai, R. Katoono, K. Fujiwara, H. Higuchi, H. Kikuchi, T. Suzuki, *Can. J. Chem*. **2017**, *95*, 243. f) C.-J. Yao, H.-J. Nie, W.-W. Yang, J.-Y. Shao, J. Yao, Y.-W. Zhong, *Chem. Eur. J.* **2014**, *20*, 17466.

[8] a) L. Wu, Y. Sun, K. Sugimoto, Z. Luo, Y. Ishigaki, K. Pu, T. Suzuki, H. Chen, D. Ye, *J. Am. Chem. Soc.* **2018**, *140*, 16340. b) L. Wu, Y. Ishigaki, Y. Hu, K. Sugimoto, W. Zeng, T. Harimoto, Y. Sun, J. He, T. Suzuki, X. Jiang, H.-Y. Chen, D. Ye, *Nat. Commun*. **2020**, *11*, 446. c) L. Wu, Y. Ishigaki, W. Zeng, T. Harimoto, B. Yin, Y. Chen, S. Liao, Y. Liu, Y. Sun, X. Zhang, Y. Liu, Y. Liang, P. Sun, T. Suzuki, G. Song, Q. Fan, D. Ye, *Nat. Commun.* **2021**, *12*, 6145. d) W. Zeng, L. Wu, Y. Ishigaki, T. Harimoto, Y. Hu, Y. Sun, Y. Wang, T. Suzuki, H.-Y. Chen, D. Ye, *Angew. Chem. Int. Ed.* **2022**, *61*, e202111759. e) L. Wu, W. Zeng, Y. Ishigaki, J. Zhang, H. Bai, T. Harimoto, T. Suzuki, D. Ye, *Angew. Chem. Int. Ed.* **2022**, *in press*. [DOI:10.1002/anie.202209248]

[9] Reviews: a) T. Suzuki, H. Higuchi, T. Tsuji, J. Nishida, Y. Yamashita, T. Miyashi, In *Chemistry of Nanomolecular Systems, Chapter 1,* Springer-Verlag, Heidelberg, **2003**; pp. 3-24. b) T. Suzuki, E. Ohta, H. Kawai, K. Fujiwara, and T. Fukushima, *Synlett* **2007**, 851. c) T. Suzuki, T. Takeda, E. Ohta, K. Wada, R. Katoono, H. Kawai, and K. Fujiwara, *Chem. Rec.* **2015**, *15*, 280. d) T. Suzuki, H. Tamaoki, J. Nishida, H. Higuchi, T. Iwai, Y. Ishigaki, K. Hanada, R. Katoono, H. Kawai, K. Fujiwara, T. Fukushima, In *Organic Redox Systems, Chapter 2*, Wiley, Hoboken, **2015**, pp.13-37. e) T. Suzuki, Y. Ishigaki, M. Takata, J. Nishida, T. Fukushima, *Heterocycles* **2021**, *102*, 419.

[10] a) S. Iwashita, E. Ohta, H. Higuchi, H. Kawai, K. Fujiwara, K. Ono, M. Takenaka, T. Suzuki, *Chem. Commun.* **2004**, 2076. b) T. Suzuki, Y. Sakano, T. Iwai, S. Iwashita, Y. Miura, R. Katoono, H. Kawai, K. Fujiwara, Y. Tsuji, T. Fukushima, *Chem. Eur. J.* **2013**, *19* 117. c) T. Suzuki, Y. Sakano, T. Iwai, S. Iwashita, Y. Miura, R. Katoono, H. Kawai, K. Fujiwara, Y. Tsuji, T. Fukushima, *Pure Appl. Chem*., **2014**, *86*, 507.

[11] Y. Ishigaki, K. Sugawara, T. Tadokoro, Y. Hayashi, T. Harimoto, T. Suzuki, *Chem. Commun*. **2021**, *57*, 7201.

[12] Y. Ishigaki, K. Sugawara, M. Yoshida, M. Kato, T. Suzuki, *Bull. Chem. Soc. Jpn.* **2019**, *92*, 1211.

[13] H. Higuchi, E. Ohta, H. Kawai, K. Fujiwara, T. Tsuji, T. Suzuki, *J. Org. Chem.* **2003**, *68*, 6605.

[14] K. S. Kim, S. H. Son, Y. H. Joo, D. Il Jung, C. S. Hahn, *Chem. Lett.* **1987**, *16*, 2251.

[15] a) A. Osuka, F. Kobayashi, K. Maruyama, *Bull. Chem. Soc. Jpn.*,**1991**, *64*, 1213. b) G. J. P. Britovsek, V. C. Gibson, O. D. Hoarau, S. K. Spitzmesser, A. J. P. White, D. J. Williams, *Inorg. Chem*. **2003**, *42*, 3454. c) J. G. Alvarado-Rodríguez, U. Hernández-Balderas, N. Andrade-López, V. Salazar, G. Sánchez-Cabrera, F. J. Zuno-Cruz, *Polyhedron* **2016**, 117, 453.

[16] a) T. Suzuki, K. Hanada, R. Katoono, Y. Ishigaki, S. Higasa, H. Higuchi, H. Kikuchi, K. Fujiwara, H. Yamada, T. Fukushima, *Chem. Lett.* **2014,** *43*, 982. b) Y. Ishigaki, H. Kawai, R. Katoono, K. Fujiwara, H. Higuchi, H. Kikuchi, T. Suzuki, *Can. J. Chem*. **2017**, *95*, 243.

[17] S. Zheng, S. Barlow, T. C. Parker, S. R. Marder, *Tetrahedron Lett.* **2003**, *44*, 7989.

[18] K. Nishio; S. Yano, Y. Kohashi, K. Yamamoto, I. Murata, *J. Am. Chem. Soc.* **1979**, *101*, 5059. b) K. Nakasuji, K. Kawamura, T. Ishihara, I. Murata, *Angew. Chem.* **1976**, *88*, 650. c) D. M. Hayes, S. D. Nelson, W. A. Garland, P. A. Kollman, *J. Am. Chem. Soc*. **1980**, *102*, 1255. d) C. Dieter; D. Bernhard; C. Dines, *J. Mol. Struc.: THEOCHEM* **1984**, *19*, 277. (thiepin, oxepin)

[19] M. J. Frisch, G. W. Trucks, H. B. Schlegel, G. E. Scuseria, M. A. Robb, J. R. Cheeseman, G. Scalmani, V. Barone, B. Mennucci, G. A. Petersson, H. Nakatsuji, M. Caricato, X. Li,H. P. Hratchian, A. F. Izmaylov, J. Bloino, G. Zheng, J. L. Sonnenberg, M. Hada, M. Ehara, K. Toyota, R. Fukuda, J. Hasegawa, M. Ishida, T. Nakajima, Y. Honda, O. Kitao, H. Nakai, T. Vreven, J. A. Montgomery, Jr., J. E. Peralta, F. Ogliaro, M. Bearpark, J. J. Heyd, E. Brothers, K. N. Kudin, V. N. Staroverov, R. Kobayashi,J. Normand, K. Raghavachari, A. Rendell, J. C. Burant, S. S. Iyengar, J. Tomasi, M. Cossi, N. Rega, J. M. Millam, M. Klene, J. E. Knox, J. B. Cross, V. Bakken, C. Adamo, J. Jaramillo, R. Gomperts, R. E. Stratmann, O. Yazyev, A. J. Austin, R. Cammi,C. Pomelli, J. W. Ochterski, R. L. Martin, K. Morokuma, V. G. Zakrzewski, G. A. Voth, P. Salvador, J. J. Dannenberg, S. Dapprich, A. D. Daniels, Ö. Farkas, J. B. Foresman, J. V. Ortiz, J. Cioslowski, D. J. Fox, Gaussian 16 (Revision A.03), Gaussian, Inc., Wallingford CT, **2016**.

[20] P. v. R. Schleyer, C. Maerker, A. Dransfeld, H. Jiao, N. J. R. E. Hommes *J. Am. Chem. Soc.* **1996**, *118*, 6317.

[21] S. Klod, E. Kleinpeter, *J. Chem. Soc., Perkin Trans. 2* **2001**, 1893.

[22] a) R. Herges, D. Geuenich, *J. Phys. Chem. A* **2001**, *105*, 3214;. b) D. Geuenich, K. Hess, F.Kohler, R. Herges, *Chem. Rev.* **2005**, *105*, 3758.

[23] Y. Ishigaki, T. Hashimoto, K. Sugawara, S. Suzuki, T. Suzuki, *Angew. Chem. Int. Ed.* **2020**, *59*, 6581.

[24] According to the DFT calculations [(U)B3LYP/6-31G(d)], the optimized geometry for **III**$^{2\bullet}$ was found at the relative energy of 7.873 kcal mol^{-1} to **III**, which is estimated to have a biradical index (y_0) of 38%. On the other hand, no energy-minimized geometry corresponding to **1**$^{2\bullet}$ was obtained. Actually, VT-^{1}H NMR measurements of **1** and **2** in DMSO-d_6 showed no line-broadening up to 393 K (Figures S3 and S4).

[25] A. Bondi, *J. Phys. Chem.* **1964**, *86*, 441.

[26] NBO Version 7.0, E. D. Glendening, J. K. Badenhoop, A. E. Reed, J. E. Carpenter, J. A. Bohmann, C. M. Morales, P. Karafiloglou, C. R. Landis, F. Weinhold, **2018**, Theoretical Chemistry Institute, University of Wisconsin, Madison, WI

[27] Y. Ishigaki, T. Harimoto, K. Sugawara, T. Suzuki, *J. Am. Chem. Soc.* **2021**, *143*, 3306.

Entry for the Table of Contents

Insert graphic for Table of Contents here.

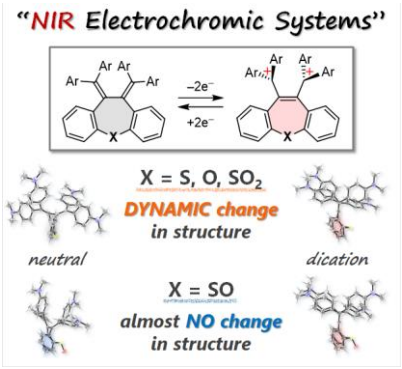

Dibenzothiepin-based redox pair and its analogues exhibit an electrochomic behavior with drastic change in the UV-Vis-NIR absorption, thus suitable for developing new bioimaging protocols. The structural change of the central seven-membered ring was found to be the key to gain electrochemical bistability upon two-electron transfer nearly at the same potential.

Twitter usernames: Yusuke Ishigaki (@ysk_isgk); Takanori Suzuki (@Yuuichi_Hokudai)